Landsat-derived Spring and Autumn Phenology, Eastern US - Canadian Forests, 1984-2013

Documentation Revision Date: 2018-04-02

Data Set Version: 1

Summary

This dataset provides Landsat phenology algorithm (LPA) derived start and end of growing seasons (SOS and EOS) at 500-m resolution for deciduous and mixed forest areas of 75 selected Landsat sidelap regions across the Eastern United States and Canada. The data are a 30-year time series (1984-2013) of derived spring and autumn phenology for forested areas of the Eastern Temperate Forest, Northern Forest, and Taiga ecoregions.

This dataset provides Landsat phenology algorithm (LPA) derived start and end of growing seasons (SOS and EOS) at 500-m resolution for deciduous and mixed forest areas of 75 selected Landsat sidelap regions across the Eastern United States and Canada. The data are a 30-year time series (1984-2013) of derived spring and autumn phenology for forested areas of the Eastern Temperate Forest, Northern Forest, and Taiga ecoregions.

The study used Landsat TM/ETM+ images acquired between 1984 and 2013 for 75 Landsat sidelap regions. Sidelaps were selected using a stratified random sampling approach within three United States Environmental Protection Agency Level I ecoregions: Northern Forest, Taiga, and Eastern Temperate Forest. The Landsat phenology algorithm (LPA) (Melaas et. al, 2013, 2016) was used to estimate the day of year (DOY) associated with leaf emergence at the start of the growing season (SOS) and autumn senescence at the end of growing seasons (EOS) for deciduous and mixed forest 30-m Landsat pixels. Data were aggregated to 500-m spatial resolution using the MODIS grid.

Additional data include the number of years of detected mean Landsat-detected spring onset and autumn onset dates, subsequent trend magnitude (Theil-Sen) and significance (Mann-Kendall) values, as well as location information including Landsat tile numbers, MODIS pixel coordinates, and ecoregion.

This dataset includes 75 files with phenology data in comma-separated (.csv) format and one shapefile (.shp) with the ecoregions locations. The shapefile is also provided in *.kmz format for viewing in Google Earth.

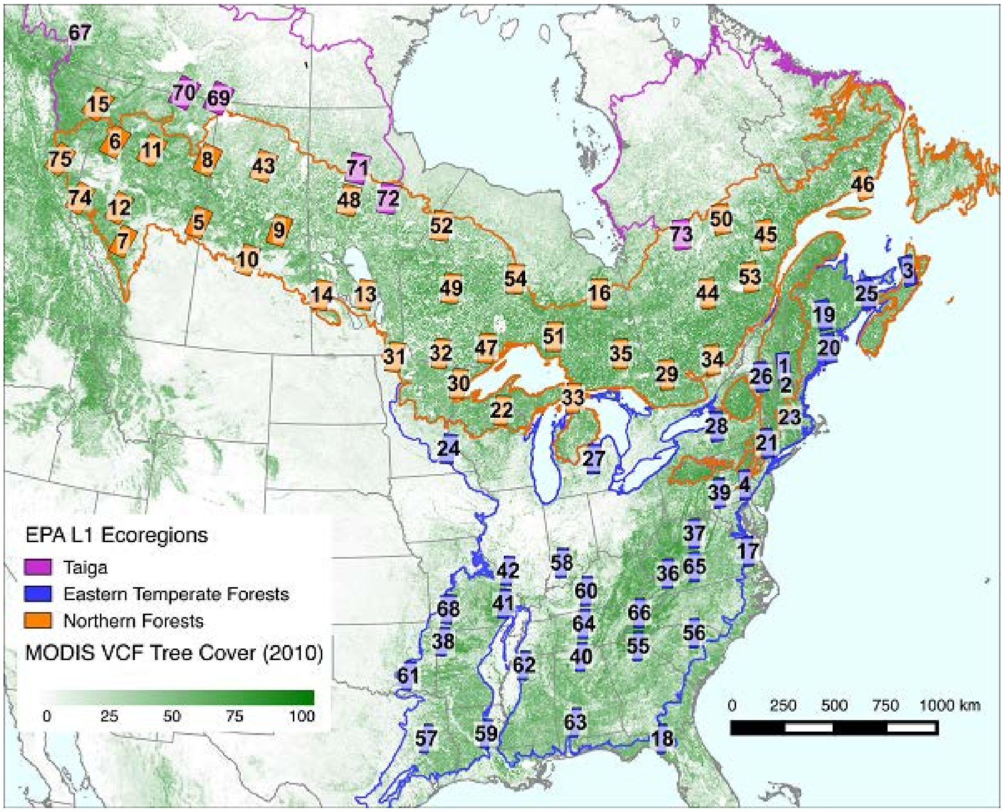

Figure 1. Map of the 75 selected Landsat sidelap regions within the three United States Environmental Protection Agency Level I ecoregions. From Melaas et al., 2018.

Citation

Melaas, E.K., M.A. Friedl, and D. Sulla-Menashe. 2018. Landsat-derived Spring and Autumn Phenology, Eastern US - Canadian Forests, 1984-2013. ORNL DAAC, Oak Ridge, Tennessee, USA. https://doi.org/10.3334/ORNLDAAC/1570

Table of Contents

1. Data Set Overview

The study used Landsat TM/ETM+ images acquired between 1984 and 2013 for 75 Landsat sidelap regions. Sidelaps were selected using a stratified random sampling approach within three United States Environmental Protection Agency Level I ecoregions: Northern Forest, Taiga, and Eastern Temperate Forest. The Landsat phenology algorithm (LPA) (Melaas et. al, 2013, 2016) was used to estimate the day of year (DOY) associated with leaf emergence at the start of the growing season (SOS) and autumn senescence at the end of growing seasons (EOS) for deciduous and mixed forest 30-m Landsat pixels. Data were aggregated to 500-m spatial resolution using the MODIS grid.

Additional data include the number of years of detected mean Landsat-detected spring onset and autumn onset dates, subsequent trend magnitude (Theil-Sen) and significance (Mann-Kendall) values, as well as location information including Landsat tile numbers, MODIS pixel coordinates, and ecoregion.

What is a sidelap? For Landsat satellites to provide nearly complete coverage of the Earth's surface with 185-km wide image swaths (later Landsats have wider swaths), some overlapping of orbits was required. The amount of swath overlap **or sidelap** varies from 7-14 percent at the Equator to a maximum of approximately 85 percent at 81 degrees north or south latitude. In these areas where overlap or sidelap occurred, more images are available, and this increases the likelihood that more good quality images (i.e., no clouds) will be available for analyses.

Related Publication

Melaas, E. K., M. A. Fridel, and D. Sulla-Menashe. 2018. Multidecadal Changes and Interannual Variation in Springtime Phenology of North American

Temperate and Boreal Deciduous Forests. Geophysical Research Letters. https://doi.org/10.1002/2017GL076933

Related Datasets

Elmore, A.J., D. Nelson, S.M. Guinn, and R. Paulman. 2017. Landsat-based Phenology and Tree Ring Characterization, Eastern US Forests, 1984-2013. ORNL DAAC, Oak Ridge, Tennessee, USA. http://dx.doi.org/10.3334/ORNLDAAC/1369

2. Data Characteristics

Spatial Coverage: Eastern United States and Canada

Spatial Resolution: 500-m

Temporal Coverage: 1984-01-01 to 2013-12-31

Temporal Resolution: Annual

Study Areas (All latitude and longitude given in decimal degrees)

Site	Westernmost Longitude	Easternmost Longitude	Northernmost Latitude	Southernmost Latitude
Eastern US and Canada	-124.424	-60.3954	62.0367	29.6345

Data File Information

SOS and EOS Timeseries Data

There are 75 files in comma-separated format (.csv), one for each of the selected sidelap regions across the Eastern United States and Canada

Each file provides the following data for a specific slidelap region:

- Each row represents a 500-m MODIS pixel with identified deciduous and mixed forest 30-m Landsat pixels. Thus, each row in a file corresponds to a potential 30-year timeseries of mean SOS and EOS as DOY for the MODIS pixel.
- But, many MODIS pixels have no (zero) Landsat pixels where SOS and EOS could be detected and all spring and autumn DOY columns are “NA”.
- For MODIS pixels with Landsat pixels where SOS and EOS could be derived for some years, those yearly spring and autumn values are the mean SOS and EOS as Julian days of those forest 30-m Landsat pixels as aggregated to a 500-m MODIS pixel for that year, potentially years 1984 through 2013.
- Together then, all the rows in a file are all the MODIS pixels in the sidelap region with identified deciduous and mixed forest Landsat pixels.
- Coordinates (centroids) and MODIS grid identifiers are provided for each MODIS pixel.
- For MODIS pixels with Landsat pixels where SOS and EOS could be derived, the total number of years of available data for spring and for autumn in the row are provided.
- Trend analysis magnitude (Theil-Sen) and significance (Mann-Kendall) values are included for SOS and EOS timeseries.

File naming conventions

The files are named as **phenology_sceneX_site_YYY_name.csv**

Where:

_sceneX is the sidelap number

_site_YYY is the Level 2 Ecoregion, and

_name refers to a location for reference purposes (forest name, town, or other location) in the sidelap.

Refer to Table 2 for the ecoregions and Table 3 for locations of the sidelaps.

Example file name:

phenology_scene23_site_mwp_harvard.csv

This file provides data for scene 23, a mixed wood plains Level 2 Ecoregion in the Harvard Forest.

Data Dictionary

Any missing data denotes that either SOS or EOS phenology dates were undetectable due to missing or poor quality Landsat imagery during the greenup and greendown periods when phenology dates are typically detected. **Missing data are indicated with NA.**

Table 1. Variables in the .csv data files

Column name	Units	Description

latitude	Decimal degrees	Latitude of the 500-m MODIS pixel centroid
longitude	Decimal degrees	Longitude of the 500-m MODIS pixel centroid
tile_h		Corresponding horizontal MODIS tile of 500-m pixel
tile_v		Corresponding vertical MODIS tile of 500-m pixel
line		Line number of MODIS pixel
samp		Sample number of MODIS pixel
tile		Corresponding MODIS tile name
num_pix	count	Number of deciduous and mixed forest 30-m Landsat pixels located within the 500-m MODIS pixel
num_spr	count	Number of years of LPA detected SOS
num_aut	count	Number of years of LPA detected EOS
spr_1984 to spr_2013 (30 columns)	DOY	Detected SOS date (Julian day of year). Value is mean SOS of forest 30-m Landsat pixels as aggregated to a 500-m MODIS pixel for that year, potentially 1984 through 2013.
aut_1984 to aut_2013 (30 columns)	DOY	Detected EOS date (Julian day of year). Value is mean EOS of forest 30-m Landsat pixels as aggregated to a 500-m MODIS pixel for that year, potentially 1984 through 2013.
ts_spr		Theil-Sen trend magnitude estimate for spring phenology time series
mk_spr		Mann-Kendall trend significance for spring phenology time series;
ts_aut		Theil-Sen trend magnitude estimate for autumn phenology time series
mk_aut		Mann-Kendall trend significance for autumn phenology time series

Table 2. EPA Level 1 and Level 2 Ecoregions in the 75 sidelaps

Level 1 Ecoregion Code	Level 1 Ecoregion	Level 2 Ecoregion Code	Level 2 Ecoregion
ETF	Eastern Temperate Forest	AH	Atlantic Highlands
ETF	Eastern Temperate Forest	MA	Mid Atlantic Coastal Plain
ETF	Eastern Temperate Forest	MWP	Mixed Wood Plains
ETF	Eastern Temperate Forest	OA	Ozark/Ouachita Appalachian Forest
ETF	Eastern Temperate Forest	SUP	Southeastern USA Plains
ETF	Eastern Temperate Forest	TEP	Temperate Prairies
NF	Northern Forest	BP	Boreal Plain
NF	Northern Forest	HP	Hudson Plain
NF	Northern Forest	MWP	Mixed Wood Plains
NF	Northern Forest	MWS	Mixed Wood Shield
NF	Northern Forest	TS	Taiga Shield
NF	Northern Forest	WC	Western Cordillera
T	Taiga	TC	Taiga Cordillera
T	Taiga	TP	Taiga Plain

T	Taiga	TS	Taiga Shield

Table 3. Characteristics of sidelap scenes. The scene locations are intended to serve as a general reference to the country and state or province and the ecoregions. Included for each scene is the "site_YYY_name" used in the respective data file name.

Scene #	Scene Reference Location	State or Province, Country	Level 1 Ecoregion	Level 2 Ecoregion	site_YYY_name
1	Bartlett	New Hampshire, USA	ETF	AH	ah_bartlett
2	Hubbard	New Hampshire, USA	ETF	AH	ah_hubbard
3	Nova Scotia	Nova Scotia, CA	ETF	AH	ah_nova_scotia
4	Philadelphia	Pennsylvania, USA	ETF	AH	ah_philadelphia
5	Bonnyville	Alberta, CA	NF	BP	bp_bonnyville
6	Chinchaga	Alberta, CA	NF	BP	bp_chinchaga
7	Edmonton	Alberta, CA	NF	BP	bp_edmonton
8	Fort Mcmurray	Alberta, CA	NF	BP	bp_fort_mcmurray
9	La Ronge	Saskatchewan, CA	NF	BP	bp_la_ronge
10	Saskatoon	Saskatchewan, CA	NF	BP	bp_saskatoon
11	Wabasca	Alberta, CA	NF	BP	bp_wabasca
12	Whitecourt	Alberta, CA	NF	BP	bp_whitecourt
13	Winnipeg	Manitoba, CA	NF	BP	bp_winnipeg
14	Yorkton	Manitoba, CA	NF	BP	bp_yorkton
15	Zama	British Columbia, CA	NF	BP	bp_zama
16	Kesagami	Ontario, CA	NF	HP	hp_kesagami
17	Chesapeake	Virginia, USA	ETF	MA	ma_chesapeake
18	Tallahassee	Florida, USA	ETF	MA	ma_tallahassee
19	Acadia	New Brunswick, CA	ETF	MWP	mwp_acadia
20	Bar Harbor	Maine, USA	ETF	MWP	mwp_bar_harbor
21	Cary	New York, USA	ETF	MWP	mwp_cary
22	Green Bay	Wisconsin, USA	NF	MWP	mwp_green_bay
23	Harvard	Massachusetts, USA	ETF	MWP	mwp_harvard
24	Minneapolis	Minnesota, USA	ETF	MWP	mwp_minneapolis
25	Moncton	New Brunswick, CA	ETF	MWP	mwp_moncton
26	Proctor	Vermont, USA	ETF	MWP	mwp_proctor
27	Saginaw	Michigan, USA	ETF	MWP	mwp_saginaw
28	Syracuse	New York, USA	ETF	MWP	mwp_syracuse
29	Algonquin	Ontario, CA	NF	MWS	mws_algonquin
30	Boundary Waters	Minnesota, USA	NF	MWS	mws_boundary_waters

31	Grand Forks	Minnesota, USA	NF	MWS	mws_grand_forks
32	Kabetogama	Ontario, CA	NF	MWS	mws_kabetogama
33	Mackinac	Michigan, USA	NF	MWS	mws_mackinac
34	Ottawa	Ontario, CA	NF	MWS	mws_ottawa
35	Sudbury	Ontario, CA	NF	MWS	mws_sudbury
36	Charleston	West Virginia, USA	ETF	OA	oa_charleston
37	Dolly Sods	West Virginia, USA	ETF	OA	oa_dolly_sods
38	Fayetteville	Arkansas, USA	ETF	OA	oa_fayetteville
39	Harrisburg	Pennsylvania, USA	ETF	OA	oa_harrisburg
40	Huntsville	Alabama, USA	ETF	OA	oa_huntsville
41	Mark Twain	Missouri, USA	ETF	OA	oa_mark_twain
42	St Louis	Illinois, USA	ETF	OA	oa_st_louis
43	Cree	Saskatchewan, CA	NF	SS	ss_cree
44	Gouin	Quebec, CA	NF	SS	ss_gouin
45	Manicouagan	Quebec, CA	NF	SS	ss_manicouagan
46	Mingan	Quebec, CA	NF	SS	ss_mingan
47	Nipigon	Ontario, CA	NF	SS	ss_nipigon
48	Nobs	Manitoba, CA	NF	SS	ss_nobs
49	Pipestone	Ontario, CA	NF	SS	ss_pipestone
50	Pletipi	Quebec, CA	NF	SS	ss_pletipi
51	Pukaskwa	Ontario, CA	NF	SS	ss_pukaskwa
52	Sachigo	Ontario, CA	NF	SS	ss_sachigo
53	Saguenay	Quebec, CA	NF	SS	ss_saguenay
54	Winisk	Ontario, CA	NF	SS	ss_winisk
55	Atlanta	Georgia, USA	ETF	SUP	sup_atlanta
56	Charlotte	South Carolina, USA	ETF	SUP	sup_charlotte
57	Davy Crockett	Texas, USA	ETF	SUP	sup_davy_crockett
58	Indianapolis	Indiana, USA	ETF	SUP	sup_indianapolis
59	Kisatchie	Louisiana, USA	ETF	SUP	sup_kisatchie
60	Mammoth Cave	Kentucky, USA	ETF	SUP	sup_mammoth_cave
61	Mcalester	Oklahoma, USA	ETF	SUP	sup_mcalester
62	Memphis	Mississippi, USA	ETF	SUP	sup_memphis
63	Montgomery	Alabama, USA	ETF	SUP	sup_montgomery
64	Nashville	Tennessee, USA	ETF	SUP	sup_nashville

65	Roanoke	Virginia, USA	ETF	SUP	sup_roanoke
66	Smoky Purchase	Tennessee, USA	ETF	SUP	sup_smoky_purchase
67	Nahanni	Northwest Territories, CA	T	TC	tc_nahanni
68	Springfield	Missouri, USA	ETF	TEP	tep_springfield
69	Athabasca	Northwest Territories, CA	T	TP	tp_athabasca
70	Slave	Northwest Territories, CA	T	TP	tp_slave
71	Amisk	Manitoba, CA	T	TS	ts_amisk
72	Gillam	Manitoba, CA	T	TS	ts_gillam
73	Mistassini	Quebec, CA	T	TS	ts_mistassini
74	Wc Kakwa	Alberta, CA	NF	WC	wc_kakwa
75	Wc Williston	British Columbia, CA	NF	WC	wc_williston

Shapefile with sidelap locations

The shapefile is provided in the compressed file **Phenology_Landsat_Sidelap_Regions_US_CA.zip.** The data are also provided as a companion file in .kmz format for viewing in Google Earth.

The shapefile provides the 75 sidelaps (scenes), as polygons. Bounding boxes for the scenes can be extracted from the scene polygons in the Shapefile.

Table 4. Attributes in the shapefile **Phenology_Landsat_Sidelap_Regions_US_CA**

Attribute	Description
FID	Number of sites (1-75)
Scene: X_location	Corresponds to locations in the broader ecoregions. The X corresponds to the abbreviation for the level 2 ecoregion of the location. Refer to Table 3. Example: ah_bartlett
L1	Level 1 ecoregion associated with each scene (sidelap). Refer to Table 3.

3. Application and Derivation

Results from this work support the utility of land surface phenology information derived from Landsat for improving information and understanding of ecosystem processes at landscape scales.

4. Quality Assessment

The assessment and validation of remotely sensed estimates of SOS and EOS dates with the Landsat phenology algorithm (LPA) was reported in Melaas et al. (2016).

5. Data Acquisition, Materials, and Methods

Overview

The Landsat phenology algorithm (LPA) described by Melaas et al. (2013) and subsequently refined and validated in Melaas et al. (2016) was used to estimate the long-term average and the annual day of year (DOY) associated with leaf emergence (start of growing season: SOS) and autumn senescence (end of growing season: EOS) at 30-m spatial resolution from time series of Landsat 4, 5, and 7 images. This study used the LPA to focus on retrieval and analysis of SOS and EOS detection for forest pixels (Melaas et al., 2018).

What is a sidelap? For Landsat satellites to provide nearly complete coverage of the Earth's surface with 185-km wide image swaths (later Landsats have wider swaths), some overlapping of orbits was required. The amount of swath overlap **or sidelap** varies from 7-14 percent at the Equator to a maximum of approximately 85 percent at 81 degrees north or south latitude. In these areas where overlap or sidelap occurred, more images are available, and this increases the likelihood that more good quality images (i.e., no clouds) will be available for analyses.

Site Selection

Data used were Landsat TM/ETM+ imagery acquired between 1984 and 2013 for 75 Landsat sidelaps located in the Eastern United States and Canada. Landsat sidelaps were selected using a stratified random sampling of sidelaps located within the United States Environmental Protection Agency Level I ecoregions (https://www.epa.gov/eco-research/ecoregions): Northern Forest, Taiga, and Eastern Temperate Forest. To provide a balanced sample representative of forested areas across these three large and heterogeneous ecoregions, the number of sites (sidelaps) was allocated based on the forested area of each Level II ecoregion located within each of the three Level I ecoregions identified above, subject to the constraint that each sidelap included in the sample has at least 10% forest cover.

To exclude areas not classified as either deciduous broadleaf forest or mixed forest, the National Land Cover Database (circa 2006) and the Earth Observation for Sustainable Developments of Forest Land Cover (circa 2000) maps (Wulder et al., 2008; Xian et al., 2009) were used. The Continuous Change Detection and Classification algorithm (Zhu & Woodcock, 2014) was used to identify and exclude pixels that experienced disturbance before 1999 or that had more than two disturbance events during the 30-year Landsat record. To avoid spurious trends in the timing of SOS associated with long-term greening and browning the EVI time series was normalized at each pixel to have unit amplitude each year using the 10^{th} and 90^{th} percentiles at each pixel based on moving three-year windows.

Estimating SOS and EOS

Average SOS and EOS were estimated using the LPA at each pixel based on the day of year when the spring and autumn logistic functions reached 50% of their amplitude (Melaas et al., 2013).

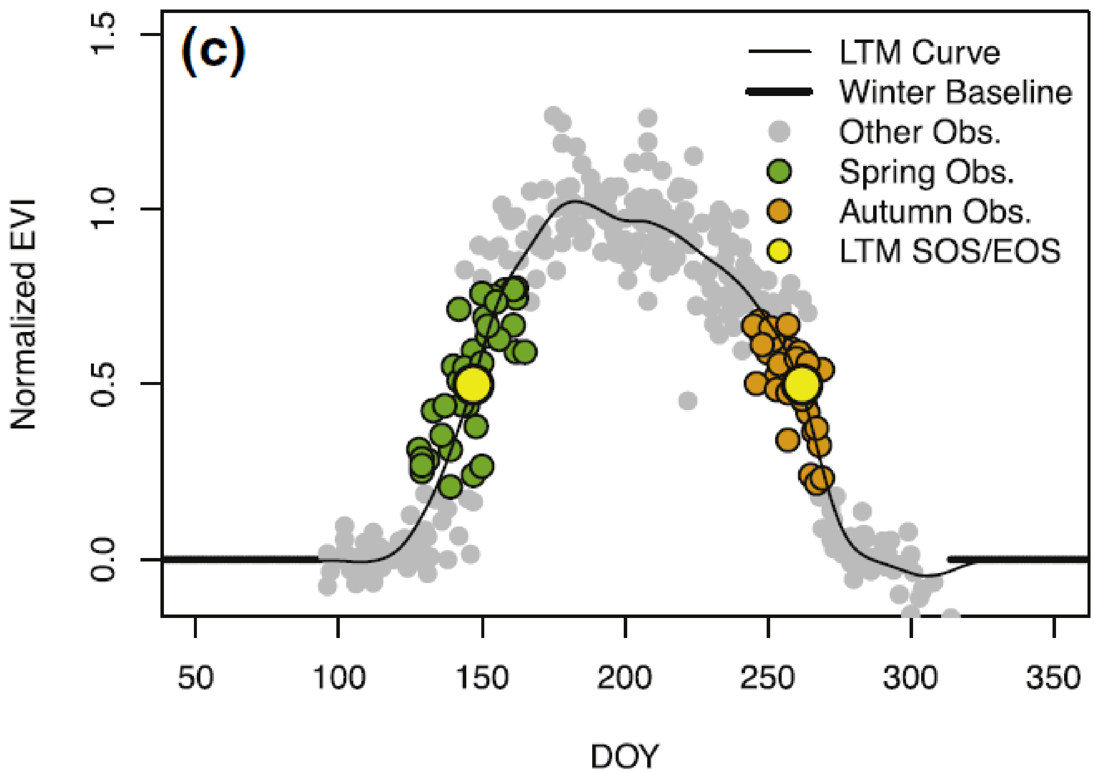

Figure 2. Example of LPA results for a sample deciduous forest 30-m Landsat pixel. Normalized EVI with long-term mean spline curve, long-term mean (LTM) transition dates (yellow dots) and in annual SOS and EOS, (green and orange dots, respectively). From Melaas et al., (2016).

Detection of SOS was not always possible at every pixel in every year because of persistent cloud cover during the springtime at some sites in some years, especially in eastern boreal Canada, which tends to be quite cloudy. To overcome this constraint, SOS time series were analyzed based on data that were up-scaled to **the MODIS grid at 500-m spatial resolution** using the mean 30-m SOS in each 500-m cell in each year. To ensure robust estimation of trends, 500-m cells were excluded with fewer than five forested Landsat pixels or for which fewer than 10 years of SOS retrievals were available.

The resulting dataset included nearly 1.2 million 500-m cells, where each grid cell provided a unique time series of SOS between 1984 and 2013. Using these time series, SOS trends were evaluated by computing the Theil-Sen slope (Sen, 1968) to estimate the magnitude of long-term SOS change, and then identified grid cells with statistically significant trends ($p < 0.05$) using the Mann-Kendall test (Mann, 1945).

Refer to Melaas et al. (2018) for additional details.

6. Data Access

These data are available through the Oak Ridge National Laboratory (ORNL) Distributed Active Archive Center (DAAC).

Landsat-derived Spring and Autumn Phenology, Eastern US - Canadian Forests, 1984-2013

Contact for Data Center Access Information:

- E-mail: uso@daac.ornl.gov
- Telephone: +1 (865) 241-3952

7. References

Melaas, E. K., M. A. Fridel, and D. Sulla-Menashe. 2018. Multidecadal Changes and Interannual Variation in Springtime Phenology of North American Temperate and Boreal Deciduous Forests. Geophysical Research Letters. https://doi.org/10.1002/2017GL076933

Melaas, E. K., Sulla-Menashe, D., Gray, J. M., Black, T. A., Morin, T. H., Richardson, A. D., & Friedl, M. A. (2016). Multisite analysis of land surface phenology in North American temperate and boreal deciduous forests from Landsat. Remote Sensing of Environment, 186, 452–464. https://doi.org/10.1016/j.rse.2016.09.014

Melaas, E. K., M.A. Friedl, M. A., and Zhu, Z. (2013). Detecting interannual variation in deciduous broadleaf forest phenology using Landsat TM/ETM + data. Remote Sensing of Environment, 132, 176–185. https://doi.org/10.1016/j.rse.2013.01.011

Sen, P. K. (1968). Estimates of the Regression Coefficient Based on Kendall's Tau. Journal of the American Statistical Association, 63(324), 1379–1389. https://doi.org/10.1080/01621459.1968.10480934

Wulder, M. A., White, J. C., Cranny, M., Hall, R. J., Luther, J. E., Beaudoin, A., Goodenough, D.G., and Dechka, J. A. (2008). Monitoring Canada's forests. Part 1: Completion of the EOSD land cover project. Canadian Journal of Remote Sensing, 34(6), 549–562. https://doi.org/10.5589/m08-066

Xian, G., Homer, C., & Fry, J. (2009). Updating the 2001 National Land Cover Database land cover classification to 2006 by using Landsat imagery change detection methods. Remote Sensing of Environment, 113(6), 1133–1147. https://doi.org/10.1016/j.rse.2009.02.004

Zhu, Z., & Woodcock, C. E. (2014). Continuous change detection and classification of land cover using all available Landsat data. Remote Sensing of Environment, 144, 152–171. https://doi.org/10.1016/j.rse.2014.01.011